

# Statistical analysis of relative pose of the thalamus in preterm neonates

Yi Lao<sup>1,2</sup>, Jie Shi<sup>4</sup>, Yalin Wang<sup>4</sup>, Rafeal Ceschin<sup>5</sup>, Darryl Hwang<sup>2</sup>, M.D. Nelson<sup>1</sup>, Ashok Panigrahy<sup>5</sup>, and Natasha Leporé<sup>1,2,3</sup>

<sup>1</sup>Department of Radiology, Children’s Hospital Los Angeles, Los Angeles CA, USA

<sup>2</sup>Department of Biomedical Engineering, University of Southern California, Los Angeles CA, USA

<sup>3</sup>Department of Radiology, University of Southern California, Los Angeles CA, USA

<sup>4</sup>School of Computing, Informatics, and Decision Systems Engineering, Arizona State University, Tempe, AZ, USA

<sup>5</sup>Department of Radiology, Children’s Hospital of Pittsburgh UPMC, Pittsburgh, PA, USA

**Abstract.** Preterm neonates are at higher risk of neurocognitive and neurosensory abnormalities. While numerous studies have looked at the effect of prematurity on brain anatomy, none to date have attempted to understand the relative pose of subcortical structures and to assess its potential as a biomarker of abnormal growth. Here, we perform the first relative pose analysis on a point distribution model (PDM) of the thalamus between 17 preterm and 19 term-born healthy neonates. Initially, linear registration and constrained harmonic registration were computed to remove the irrelevant global pose information and obtain correspondence in vertices. All the parameters for the relative pose were then obtained through similarity transformation. Subsequently, all the pose parameters (scale, rotation and translation) were projected into a log-Euclidean space, where univariate and multivariate statistics were performed. Our method detected relative pose differences in the preterm birth for the left thalamus. Our results suggest that relative pose in subcortical structures is a useful indicator of brain injury, particularly along the anterior surface and the posterior surface. Our study supports the concept that there are regional thalamic asymmetries in the preterm that may be related to subtle white matter injury, have prognostic significance, or be related to preterm birth itself.

## 1 Introduction

Being born prematurely is a risk factor to lifelong neurocognitive and neurosensory deficits (see e.g. [8, 13]). Abnormalities have been detected in several areas of the brain of premature newborns, including subcortical structures such as the thalamus [3, 12]. The thalamus is a ‘switch board’ structure in the brain which starts its formation as early as the 15th gestational week [5]. As a result, it is likely a sensitive indicator of prematurity, and this structure has been the focus of several brain anatomy studies associated with preterm birth. Reduced thalamic

volumes associated with preterm birth have been documented through several MRI studies [12]. In particular, [14] detected statistically significant morphological changes in the left thalamus using multivariate tensor-based morphometry (mTBM).

While maturity is a continuous process that spans the first few years of life, the first several months after birth are especially critical since the growth exhibits an outward expanding trend with evident subcortical structure changes, in terms of size, shape and relative pose within the brain. Complementary to size and shape analysis, the relative pose of subcortical structures may help to indicate the abnormal growth of the brain. This information is especially important in depicting the developing or degeneration patterns of the brain, when shifts of pose in different subcortical structures are more likely to happen. In brain degeneration studies, [1] successfully detected brain atrophy associated pose changes in Alzheimer’s disease. However, to our knowledge, few or no pose information is included in prematurity studies and relative pose has not yet been studied in relation to brain development. Here, we use similarity transformations to align the thalamus of each subject, and perform univariate as well as multivariate analyses on so-generated pose parameters, thus investigating the effect of prematurity on the relative pose between preterm and term-born neonates at term-equivalent age. We tested the hypothesis that we may detect regional differences in thalamic relative pose in preterms with no visible injury compared to term controls.

There are two major contributions in this paper. First, we developed a novel pose analysis system that integrates various brain surface processing techniques including parametrization and constrained harmonic registration and reports the subtle pose changes on subcortical structures. The obtained pose information is complementary to subcortical surface shape analyses, and the combined shape and pose results form a complete subcortical morphometry system. Secondly, we applied the system to study prematurity. Our preliminary results indicate that the pose analysis information is consistent with prior discoveries, so our work provides a novel tool for brain research in neonates.

## 2 Subjects and Methodology

### 2.1 Neonatal data

T1-weighted MRI scans consisting of 17 preterm neonates (gestational ages 25-36 weeks,  $41.12 \pm 5.08$  weeks at scan time) and 19 term born infants (gestational ages 37-40 weeks,  $45.51 \pm 5.40$  weeks at scan time) were acquired using dedicated neonatal head coils on 1.5T GE scanners, with coronal 3D spoiled gradient echo (SPGR) sequence. All the subjects in our datasets were classified into a preterm group and term group by 2 neonatal neuroradiologists. Preterm neonates included in this study were less than 37 gestational weeks at birth, and without visible injuries on MR scans. Subjects with abnormal MR scans were excluded in our datasets.

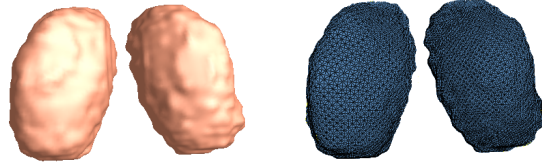


Fig. 1: 3D surface model of the left and the right thalamus and their corresponding mesh grids from one subject.

## 2.2 Point distribution model

All the T1-weighted MRI scans were first registered to a same template space through linear registration. Alignment quality was validated by superimposing images from different subjects on top of each other. Irrelevant global pose difference induced by different locations and orientations during scans was factored out in this step. The thalami were then manually traced on linear registered T1 images by an experienced pediatric neuroradiologist using Insight Toolkit’s SNAP program [16]. The intra-rater percentage overlap were 0.93 for the thalamus, in four participants at two subsequent times (two preterm and two term born participants). Based on binary segmentations, 3D surface representations of the thalamus were constructed and mesh grids were built on the surfaces by computing surface conformal parameterizations with holomorphic 1-forms, using our in-house conformal mapping program. Fig. 1 shows an example of a reconstructed surface, and corresponding mesh grids on a thalamus. One-to-one correspondence between vertices were obtained through a constrained harmonic registration algorithm [15].

## 2.3 Similarity transformation

For each thalamus, the relative pose was obtained by a full Procrustes fit of a template shape to the PDM. The template shape was selected as the mean shape that minimized the Procrustes distances, and it was computed iteratively [11]. Full Procrustes alignment means that the similarity transformation is estimated in terms of a uniform scale, a rotation and a translation in x, y and z directions [4]. To be more specific, here, the transformations were centered according to the center of mass of the mean shape. The transformation rule of Procrustes alignment is defined as [1],  $T\langle X \rangle = (sRX, d)$ , where  $s$  is the scalar scaling factor,  $R$  is a  $3 \times 3$  rotation matrix and  $d$  is the translation vector  $(x, y, z)^T$ . To form a Lie group with matrix multiplication, the matrix representation of the Procrustes transformation can be written as [2]:

$$T = \begin{pmatrix} sRX & d \\ 0^T & 1 \end{pmatrix} \quad (1)$$

To simplify computations, all the parameters of the transformations were projected onto a log-Euclidean space - the tangent plane at the origin of the

transformation group manifold. Because these similarity transformations form a Lie group, projections can be computed as matrix logarithms and exponentials as explained in [2].

In group studies, it is intuitive to define a mean. Similar to Euclidean space, here the mean in Lie group was defined as the point which minimized the squared distance [6], and the mean pose can be calculated iteratively as follow [1, 10]:

$$m_{k+1} = m_k \exp\left(\frac{1}{n} \sum_{i=1}^n \log(m_k^{-1} T_i)\right). \quad (2)$$

After the subtraction of the mean from each subject’s individual pose, specifically using  $v_i = \log(m_k^{-1} T_i)$ , each subject is left with a residual pose. Statistics are computed on the residual pose which consists of 7 parameters: 1 scale scalar, 3 rotation scalars and 3 translation scalars.

## 2.4 Statistical analysis

Although the mean and distribution of age was roughly matched between preterm and term groups, subjects were scanned over an age range of 36-57 postconception weeks. This variation of age is not negligible, especially for neonates, whose brains change rapidly with age. The distributions of 7 pose parameters are shown in Fig. 2; to save the space, only the data from the left thalamus are presented. The growth of the thalamus in neonates in terms of the volumetry and outgoing trajectory is approximately linear, thus we used linear regression to factor out the influence of age. Subsequent statistical analyses were performed on age-covariating data. It is important to note that although log S is approximately steady with age in the term group, the trend in the preterm group is saliently decreased. This is due to the existence of extremely preterm subjects (born 25-31 gestational weeks). A linear regression line of preterm data excluding the extremely preterm cases is also shown in the same panel in cyan color in Fig. 3. The line is close to constant as in the term born case.

Statistical comparisons between the two groups were performed via two methods: univariate  $t$ -test for logS,  $\|\log R\|$ ,  $\|\log d\|$ ,  $\theta_x, \theta_y, \theta_z$ , x, y, z; Multivariate Hotelling’s  $T^2$ -test, which is a multivariate generalization of the  $t$ -test, for 3 rotation parameters ( $\theta_x, \theta_y, \theta_z$ ), 3 translation parameters (x, y, z), a combination of logS,  $\|\log R\|$ , and  $\|\log d\|$ , as well as a combination of all 7 parameters.

Considering the limited size of our dataset (36 subjects), a permutation test [9] was performed to avoid the normal distribution assumption. To do this, we randomly permuted the labels of our subjects (preterm vs. term neonates), and generated  $t$ -values (for  $t$ -test) or  $F$ -values (for  $T^2$ -test) for comparison. We used 10000 permutations for each of the parameters to assemble a null distribution of nonparametric estimation for  $t$ - or  $F$ -values.

Table 1: P-value of statistical analyses on pose parameters: 13 sets of parameters characterizing relative pose of left thalamus (LTha) and right thalamus (RTha) are investigated here using univariate and multivariate analyses. Parameters are categorized as  $\log S$ ,  $||\log R||$ ,  $||\log d||$ ,  $\theta_x, \theta_y, \theta_z$ ,  $x$ ,  $y$ , and  $z$  for univariate tests, and as  $(\theta_x, \theta_y, \theta_z)$ ,  $(x, y, z)$ ,  $(\log S, ||\log R||, ||\log d||)$ , and a combination of 7 parameters for multivariate tests. All the  $p$ -values are obtained after permutation testing. Significant  $p$ -values ( $p < 0.05$ ) are highlighted in light cyan, while  $p$ -values that are interestingly low but failed to reach significance are highlighted in light grey.

|            | LTha     | RTha     |                                    | LTha     | RTha     |
|------------|----------|----------|------------------------------------|----------|----------|
| $\log S$   | 2.27e-02 | 3.43e-01 | $  \log R  $                       | 5.75e-01 | 5.73e-01 |
| $\theta_x$ | 5.60e-03 | 6.49e-01 | $  \log d  $                       | 8.88e-01 | 4.00e-01 |
| $\theta_y$ | 1.94e-01 | 9.21e-01 | $(\theta_x, \theta_y, \theta_z)$   | 9.80e-03 | 7.14e-01 |
| $\theta_z$ | 5.29e-02 | 2.61e-01 | $(x, y, z)$                        | 8.41e-01 | 8.23e-01 |
| $x$        | 4.97e-01 | 8.85e-01 | $(\log S,   \log R  ,   \log d  )$ | 1.76e-01 | 4.67e-01 |
| $y$        | 8.40e-01 | 4.85e-01 | <i>All7paras</i>                   | 2.05e-02 | 9.17e-01 |
| $z$        | 6.35e-01 | 4.90e-01 |                                    |          |          |

### 3 Results

All the  $p$ -values from previously described tests are presented in Table 1. As we can see from the table, for the left thalamus, pose parameters representing scale and rotation show a significant difference between the preterm and term groups, while no difference can be seen in translation parameters. It is also important to note that, apart from the difference detected in individual parameters, a combination of all 7 parameters also detected significant differences between the two groups in the left thalamus, indicating a possibility of using multivariate analysis of all pose parameters as the discriminant between the two populations. For the right thalamus, neither the individual or combination of parameters detected any changes.

These results are better visualized in Fig. 3, where mean shapes of preterm (represented in red) vs. term (represented in blue) groups are overlaid in their corresponding mean pose. The left thalamus of the preterm group showed a smaller size as well as an inward tendency compared to the term group, which is consistent with the differences found in scale and rotation parameters. Compared to the obvious differences in size and shape, the shift of position of the left thalamus in these two groups are less evident, thus further validating the less significant result from translation parameters. As for the right thalamus, we can see mean shapes from these 2 groups are mostly overlapped, only a slight size difference is shown in Fig. 3. These are also consistent with the relatively high  $p$ -value found in the scale, rotation and translation parameters.

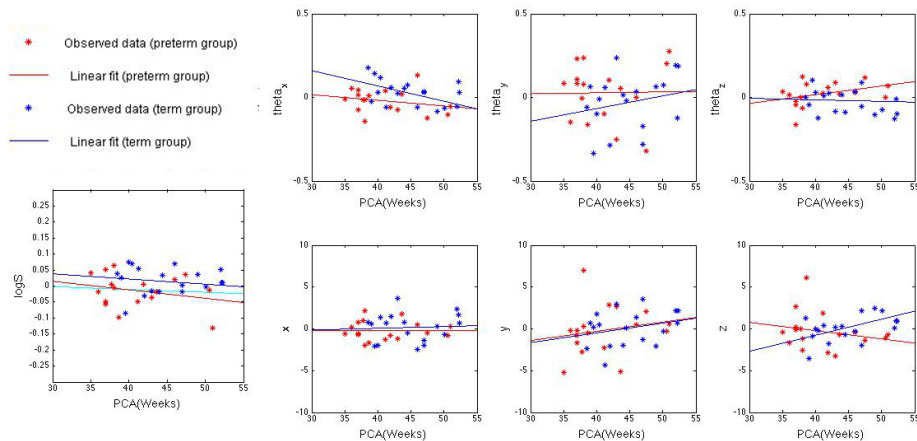


Fig. 2: Distribution of 7 pose parameters in log-Euclidean space for the left thalamus:  $\log S$ ,  $(\theta_x, \theta_y, \theta_z)$ ,  $(x, y, z)$ . Stars in the figure represent observed data from Procrustes alignment, while lines represent their corresponding linear regressions. In all the figures above, data from preterm group are marked in red, and data from term group are marked in blue. Note that  $\log S$  is approximately constant with post-conception age, indicating that the thalamus volume is near constant in that age range. However, a downward slope is seen in the preterm group. When very preterm subjects are removed from the sample (postconception age at birth  $< 31$  weeks), the linear regression (shown in a cyan) for preterm subjects normalizes to a flat line, indicating a similar behavior to the term born subjects.

## 4 Discussion

Here, we introduced a relative pose analysis into the prematurity associated brain anatomy analyses. Our pose computation successfully detected differences in the left thalamus in preterm neonates, while no difference in terms of relative pose was detected on the right thalamus between preterm and term neonates. The two thalami in the brain are not exactly symmetric in terms of functions, and hemispheric asymmetries in the thalamus have been well-documented via animal studies [7]. Our results provide additional information about the developing patterns of the two thalami.

Before our study, a reduction in thalamic volume in preterm infants compared to term-born controls was shown by manual volumetry study [12]. The reductions are consistent with the significant differences in the scale parameter we found here. However, in the volumetry study, the left and right thalami are treated as a whole, thus failing to localize the differences within the two thalami. A recent surface morphometry study has found significant regional differences on the surface of the left thalamus [14], while fewer surface changes are detected in the right thalamus. Complementary to these results, the pose information we found in our study further confirms that the left thalamus may be more vulnerable

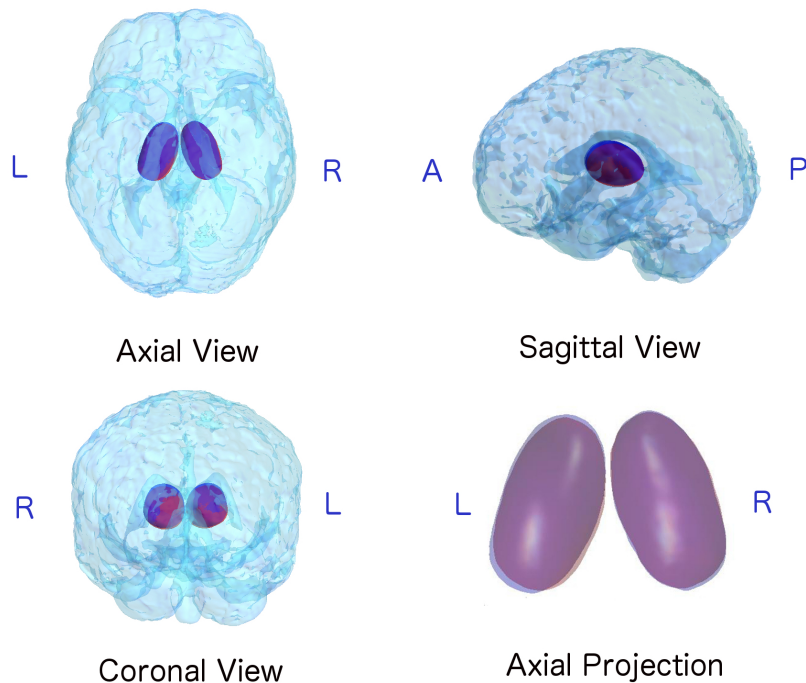


Fig. 3: 3D visualization of the pose of mean shapes averaged from preterm group (Red) and term group (Blue). The relative position of thalamus are presented in a transparent head, shown in Axial, Sagittal and Coronal views. A close look of the Axial view is shown in the bottom right corner: areas where the mean shapes of two groups overlaid appear in purple. Note the borders of these two structures: shift of pose is evident on the left thalamus, while less visible variants appear on the right thalamus. In addition, there appears to be more shifting of the anterior and posterior ends of the thalamus which co-localize to the pulvinar (posterior) and the medial dorsal and anterior nucleus (anterior).

to prematurity. In addition, the relative pose information also revealed regional differences which co-localize to known nuclear subdivision in the thalamus (i.e. pulvinar and medial dorsal nucleus) which have been previously shown to be abnormal in preterm neonates relative to term controls. Here, we demonstrate for the first time that relative pose can help with delineating regional changes of the preterm thalamus, with respect to the anterior and posterior poles of the left thalamus.

Moreover, in very preterm subjects, the scale parameter is reduced with postconception age. This supports the existence of regional vulnerability of the preterm thalamus, in the setting of no visible white matter injury. Our data suggest that even when there are global subtle volumetric difference related to the degree of prematurity, relative pose (likely in combination with surface TBM) may assist with delineating regional thalamic changes.

Our work proposes a complete set of relative pose statistics based on more accurate subcortical structure registrations: Firstly, our study used an accurate mesh representation consisting of 15,000 surface points, and point correspondences were obtained by a constrained harmonic registration, which outperforms traditional algorithms in matching the large differences between neonatal brain volumes, thus yielding higher accuracy. Secondly, post statistics are performed using both univariate and multivariate analyses on different combinations of pose parameters and their norms, to find the most sensitive statistical marker for prematurity associated differences. Finally, this is the first time that the trend of pose parameters vs. PCA has been computed. There is little research on pose in brain structure in general, and none in neonates. Our work may lead to new biomarkers for prematurity.

There are several possible limitations in this study: 1) the effect of age was removed using linear regression, however, for some of our parameters such as  $\theta_y$  and  $T_y$ ,  $T_z$  (Fig.2), the linear model may not best describe the age-dependent changes. Therefore, a more dedicated age-covariant model is needed in future studies. 2) Our study is limited to a relatively small number of subjects. We plan to increase our sample size in the future to confirm results found here, and correlating our findings with neurodevelopmental outcomes. In addition, we plan to examine the relative pose of different subcortical structures (i.e putamen, hippocampus and thalamus) in relation to reach other in preterm neonates relative to term controls, which may shed light on the global effects of prematurity on grey matter structures.

## References

1. Bossa, M., et al.: Statistical analysis of relative pose information of subcortical nuclei: application on adni data. *Neuroimage* **55**(3) (2011) 999–1008
2. Bossa, M.N., et al.: Statistical model of similarity transformations: Building a multi-object pose model of brain structures. In: *IEEE Comput. Soc. Workshop Math. Methods Biomed. Image Anal.* (2006) 59
3. Counsell, S.J., et al.: Thalamo-cortical connectivity in children born preterm mapped using probabilistic magnetic resonance tractography. *Neuroimage* **34**(3) (2007) 896–904
4. Dryden, I., et al.: *Statistical analysis of shape*. Wiley (1998)
5. Glenn, O.A.: Normal development of the fetal brain by mri. In: *Seminars in perinatology*. Volume 33., Elsevier (2009) 208–219
6. Karcher, H.: Riemannian center of mass and mollifier smoothing. *Communications on pure and applied mathematics* **30**(5) (1977) 509–541
7. King, C., et al.: Thalamic asymmetry is related to acoustic signal complexity. *Neuroscience letters* **267**(2) (1999) 89–92
8. Marlow, N., et al.: Neurologic and developmental disability at six years of age after extremely preterm birth. *New England Journal of Medicine* **352**(1) (2005) 9–19
9. Nichols, T.E., et al.: Nonparametric permutation tests for functional neuroimaging: a primer with examples. *Human brain mapping* **15**(1) (2001) 1–25
10. Pennec, X., et al.: A riemannian framework for tensor computing. *International Journal of Computer Vision* **66**(1) (2006) 41–66



11. Ross, A.: Procrustes analysis. Course report, Department of Computer Science and Engineering, University of South Carolina (2004)
12. Srinivasan, L., et al.: Quantification of deep gray matter in preterm infants at term-equivalent age using manual volumetry of 3-tesla magnetic resonance images. *Pediatrics* **119**(4) (2007) 759–765
13. Vohr, B.R., et al.: Neurodevelopmental and functional outcomes of extremely low birth weight infants in the national institute of child health and human development neonatal research network, 1993–1994. *Pediatrics* **105**(6) (2000) 1216–1226
14. Wang, Y., et al.: Surface morphometry of subcortical structures in premature neonates. In: *Proc. Intl. Soc. Mag. Reson. Med.* Volume 19. (2011) 2585
15. Wang, Y., et al.: Surface-based tbm boosts power to detect disease effects on the brain: An n= 804 adni study. *Neuroimage* **56**(4) (2011) 1993–2010
16. Zhang, H., et al.: Deformable registration of diffusion tensor mr images with explicit orientation optimization. *Medical image analysis* **10**(5) (2006) 764–785